International Journal of Applied Earth Observation and Geoinformation 34 (2015) 103–112

Contents lists available at ScienceDirect

International Journal of Applied Earth Observation and Geoinformation

journal homepage: www.elsevier.com/locate/jag

A support vector machine to identify irrigated crop types using time-series Landsat NDVI data

Baojuan Zheng[a,*], Soe W. Myint[a,c], Prasad S. Thenkabail[b], Rimjhim M. Aggarwal[c]

[a] School of Geographical Sciences and Urban Planning, Arizona State University, Tempe, AZ 85287, United States
[b] United States Geological Survey (USGS), 2255 N Gemini Dr., Flagstaff, AZ 86001, United States
[c] School of Sustainability, Arizona State University, Tempe, AZ 85287, United States

ARTICLE INFO

Article history:
Received 19 December 2013
Accepted 18 July 2014

Keywords:
Crop classification
Landsat
NDVI
Support vector machines
SVM

ABSTRACT

Site-specific information of crop types is required for many agro-environmental assessments. The study investigated the potential of support vector machines (SVMs) in discriminating various crop types in a complex cropping system in the Phoenix Active Management Area. We applied SVMs to Landsat time-series Normalized Difference Vegetation Index (NDVI) data using training datasets selected by two different approaches: stratified random approach and intelligent selection approach using local knowledge. The SVM models effectively classified nine major crop types with overall accuracies of >86% for both training datasets. Our results showed that the intelligent selection approach was able to reduce the training set size and achieved higher overall classification accuracy than the stratified random approach. The intelligent selection approach is particularly useful when the availability of reference data is limited and unbalanced among different classes. The study demonstrated the potential of utilizing multi-temporal Landsat imagery to systematically monitor crop types and cropping patterns over time in arid and semi-arid regions.

Introduction

Arizona has a warm, dry climate with two distinct wet seasons in late summer and winter (Sheppard et al., 2002). Studies show that climate change could results in more extreme weather events, such as prolonged and intense droughts in semi-arid environment (Karl et al., 2009; Overpeck and Udall, 2010). With rapidly growing population and urbanization, and the additional challenges from climate change, Arizona is facing major water-management challenges to meet human needs while maintaining ecosystem health (Gleick and Palaniappan, 2010).

Agricultural sector is a vital part of Arizona's economy; it contributed around $4 billion in value added ("Impacts of Agricultural Production", 2010). However, irrigated agriculture consumes about 68% of total water use in the state – the largest use of freshwater in Arizona (Cousteau, 2012). In the events of droughts and water scarcity, agricultural sector is projected to be impacted the most in terms of water availability in Arizona (CAST, 2009). As such, improving water use efficiency in agricultural sector is critical. Monitoring agricultural water use by crop type at different spatial scales could assist in formulating water resource management plans and policies. Furthermore, accurate site-specific information of crop types is required for detailed assessments of agricultural water use and for other agro-environmental assessments.

The potential to use remote sensing imagery for crop classification over large areas has been broadly investigated and crop phenology is the basis for cropland mapping (Chang et al., 2007; Long et al., 2013; Shao et al., 2010; Turker and Arikan, 2005; Vintrou et al., 2012; Wardlow et al., 2007; Zhong et al., 2014). The Moderate Resolution Imaging Spectroradiometer (MODIS) data has high potential for mapping crops worldwide because of its high temporal and moderate spatial resolution attributes. Using MODIS data to map crop types has been implemented across different parts of the world at a regional level (Vintrou et al., 2012; Wardlow and Egbert, 2008). There are also studies that combine MODIS data and moderate spatial resolution data, such as Landsat and the Indian Remote Sensing Advanced Wide Field Sensor (AWIFS), to discriminate crop types (Thenkabail and Wu, 2012; USDA-NASS, 2013). Other studies used higher spatial resolution imagery, such as Landsat and ASTER data, to differentiate crop types for a less extensive area (Peña-Barragán et al., 2011; Serra and Pons, 2008; Turker and Arikan, 2005). Image selection for crop type mapping largely depends on the extensiveness of the study area, image availability, the cost, and the level of diversity in crop types and management. Although both

* Corresponding author. Tel.: +1 646 750 7087.
E-mail address: bzheng11@asu.edu (B. Zheng).

http://dx.doi.org/10.1016/j.jag.2014.07.002
0303-2434/

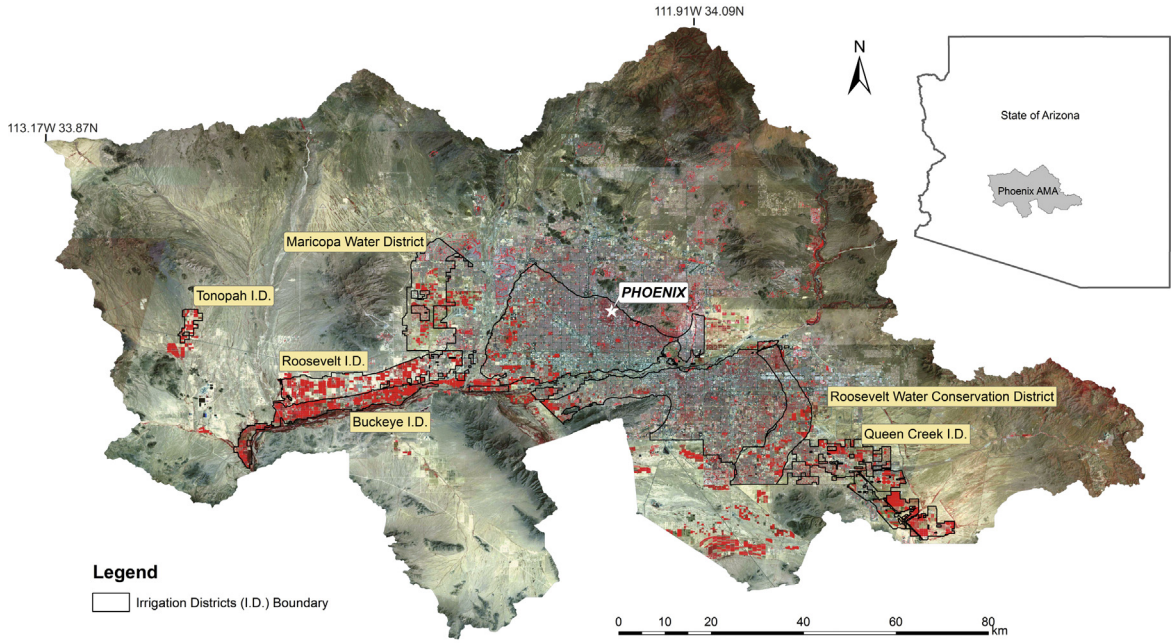

Fig. 1. False color (bands 4, 3, and 2 in red, green, and blue respectively) Landsat imagery of the Phoenix Active Management Area (PHX AMA) overlay with irrigation district boundary. (Note that some agricultural lands do not belong to any irrigation districts.). (For interpretation of the references to color in this figure legend, the reader is referred to the web version of this article.)

MODIS and Landsat data are freely available, MODIS data generally encounter a well-known mix-pixel problem due to its coarse spatial resolution (250–500 m), and the eight-day revisit rate of Landsat 5 TM and 7 EMT+ combined cannot provide enough number of cloud-free imagery for most regions in the world. However, the identification of detailed crop types in a complex agriculture management area using Landsat 30 m resolution data can be expected to be more desirable and accurate in comparison to MODIS, especially for many tropical, subtropical regions characterized by smaller agricultural fields. While most regions suffer from limited availability of could-free Landsat imagery, there are plenty in arid, semi-arid, and any dry climate regions. Leveraging this positive aspect, we attempted to effectively map crop types in Arizona, by employing frequent cloud-free Landsat observations.

Given the above background, the study aims to examine the potential of using Landsat time-series Normalized Difference Vegetation Index (NDVI) data to differentiate different crop types in the Phoenix Active Management Area (PHX AMA). The specific objectives of the study are to: (1) characterize seasonal spectral changes (i.e., NDVI temporal profiles) of different crops to assist accurate crop classification in the region; (2) evaluate the effectiveness of support vector machines (SVMs) in discriminating various crop types using a small training dataset; (3) examine if SVMs using Landsat imagery alone are capable of identifying double cropping patterns.

Investigation of these questions will provide the basis for its operational application to survey croplands over time in the PHX AMA region. One of the significant impediments in crop type mapping is the lack of quality training data (Shao et al., 2010). When ideal ground reference data is not available or limited, an alternative approach to acquire reference data is to use prior knowledge of cropping practices and spectral data collected in another year. This study, thus, also provides a direct visual comparison between crop types and NDVI time-series spectral profiles, and information on crop management, to assist acquisitions of high-quality training data. Such information is important for long-term, local, and global cropland mapping efforts (Thenkabail et al., 2012), especially when there is limited availability of ground reference data.

Support vector machine classifier

Support vector machine (SVM) classifier is a non-parametric supervised classification derived from statistical learning theory. SVM was developed in the late 1970s, but its popularity in remote sensing only began to increase about a decade ago (Mountrakis et al., 2011). The underlying theory and detailed mathematical explanation of SVM have been demonstrated in many previous studies (Ben-Hur and Weston, 2010; Foody and Mathur, 2004; Vapnik, 1999). SVM training algorithm maps the training data into higher dimensional space and finds the optimal hyperplanes that separate classes with minimum classification errors. The optimal hyperplanes are positioned using training samples that lie at the edges of class distribution in a feature space. The training samples that define the hyperplane of maximum margin are called support vectors. All the other training samples do not make any contribution to estimate hyperplane locations, and therefore can be discarded (Belousov et al., 2002; Brown et al., 2000). Consequently, it is possible to use SVM to achieve high classification accuracy using a small number of training samples.

Similar to other non-parametric classifiers, SVM does not assume that data is normally distributed for a particular image. This allows SVM to perform better than techniques based on maximum likelihood classification (Bruzzone and Persello, 2009; Dalponte et al., 2008). Previous studies showed that SVM has the ability to generalize to unseen data with a small training dataset (Foody and Mathur, 2004; Plaza et al., 2009; Shao and Lunetta, 2012). Shao and Lunetta (2012) compared SVM to two other non-parametric classifiers, i.e., neural networks (NN), and classification and regression trees (CART). They found that SVM achieved substantially higher classification accuracy than NN and CART using a small training sample size (i.e., 20 pixels per class) (Shao and Lunetta, 2012). SVM is an appealing approach to handle high-dimensional data with a limited training set (Plaza et al., 2009). It was applied to time-series MODIS (Carrão et al., 2008; Shao and Lunetta, 2012) and RapidEye (Löw et al., 2013) data. However, to our best knowledge, SVM has not yet been applied to time-series Landsat data to classify different crop types.

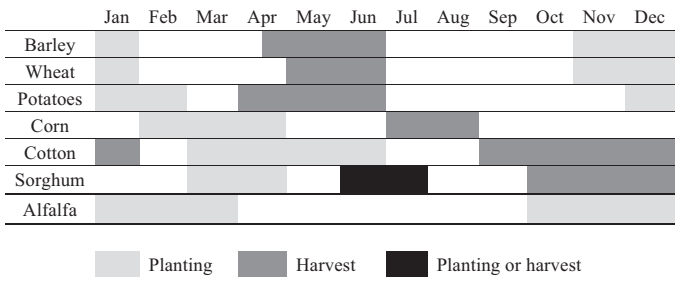

Fig. 2. Usual planting and harvest dates of the crops grown in the region (USDA-NASS, 2004).

Study area

We conducted our study in the PHX AMA in Central Arizona (Fig. 1). The PHX AMA has a subtropical desert climate with average annual temperature of 22.72 °C and a bimodal seasonal rainfall pattern with most rainfall occurring from December to March and from July to September (USDA-NRCS, 2013). The average annual precipitation is 203 mm (ADWR, 2012a). Thus, the area relies on irrigation for farming, which accounted for about 47% of all the water used in PHX AMA during the period from 2001 to 2005 (ADWR, 2012b). Because of the warm climatic conditions, farmers grow a variety of crops all around the year. Major field crops in this area are alfalfa, durum wheat, barley, cotton, corn, and sorghum. Barley and wheat are spring crops, which are harvested before June; while cotton, corn, and sorghum are summer crops. Usual planting and harvest dates for these crops are presented in Fig. 2. Among these crops, alfalfa, cotton, and corn are highly water intensive. Farmers also grow potatoes, melons, and a variety of vegetables (such as carrots, lettuce, and broccoli). Alfalfa, other hay, and vegetables can be grown year round. It is common that growers practice double cropping for field crops and multiple cropping for vegetable crops in this region. Planting crops in late fall (October–December) and harvesting in the next spring is also practiced. The cropping system in the study area is thus highly varied. Crop types and farm management practices differ significantly across the irrigation districts, due to varied soil salinity levels and the quantity and quality of water available. For example, growers can cultivate low salt tolerant crops, such as watermelon, flowers, and vegetables, in Maricopa Water District, benefiting from the good water quality supplied from the Agua Fria River. In contrast, the majority of lands in Buckeye Irrigation District, however, are only suitable for growing more salt tolerant crops, such as alfalfa, durum wheat, and sorghum.

Materials and methods

Remotely sensed data

Because of the dry climate conditions, there is an abundance of cloud-free Landsat imagery available for our study area. A total of 24 scenes of Landsat 5 TM and 7 ETM+ (Path 37/Row 37) for 2010 (Table 1) were atmospherically corrected to surface reflectance using the Landsat Ecosystem Disturbance Adaptive Processing System (LEDAPS) (Masek et al., 2006). We then generated NDVI layers for each image. There are a total of 14 scenes of Landsat 7 ETM + images. Landsat 7 ETM + images have data gaps since the scan line corrector (SLC) failed in 2003. We filled Landsat 7 missing data using procedures described in Section "Gap-filling Landsat 7 missing NDVI data". Three images acquired on day of year (DOY) 153, 185, and 193 were partially contaminated by clouds (<10%). Two scenes acquired within ≤8-day windows were paired (i.e., DOY 153 and 161; DOY 185 and 193) and the maximum NDVI values were extracted for each image pair to remove cloud contaminated pixels. Subsequently, a total of 22 NDVI layers spanning from January 9 (day 9) to December 11 (day 345) were stacked to produce a time-series Landsat NDVI image. The purpose of gap-filling and cloud elimination procedures is to reduce data noise.

Table 1
Availability of Landsat imagery (Path 37/Row 27) with less than 5% clouds from 2000 to 2010.

Year	Landsat sensor	Acquisition dates (day of year)	Total number of scenes
2010	5 TM	49, 97, 145, 161, 177, 193, 225, 257, 305, 321	10
	7 ETM+	9, 25, 73, 89, 105, 121, 153, 169, 185, 217, 281, 313, 329, 345	14
2009	5 TM	14, 30, 94, 110, 126, 190, 222, 238, 254, 270,	10
	7 ETM+	6, 70, 86, 102, 134, 150, 166, 230, 294, 326, 343, 358	12
2008	5 TM	60, 92, 108, 124, 140, 172, 236, 284, 300, 316	10
	7 ETM+	20, 36, 52, 84, 116, 132, 148, 164, 212, 276, 292, 308, 324, 340, 356	15
2007	5 TM	25, 57, 73, 89, 105, 137, 169, 233, 273,	9
	7 ETM+	1, 17, 33, 97, 129, 177, 193, 241, 289, 305, 321, 337, 353	13
2006	5 TM	22, 102, 134, 150, 166, 214, 262, 294, 310, 342	10
	7 ETM+	30, 46, 62, 110, 126, 190, 238, 270, 334,	9
2005	5 TM	19, 67, 131, 163, 179, 195, 227, 243, 259, 275, 323	11
	7 ETM+	59, 75, 91, 107, 123, 139, 155, 187, 267, 283, 299, 363	12
2004	5 TM	17, 97, 113, 145, 161, 177, 193, 209, 241, 257, 273,321, 337, 353	14
	7 ETM+	9, 41, 57, 89, 105, 121, 137, 153, 169, 185, 201, 265, 281, 297, 345	15
2003	5 TM	14, 30, 78, 94, 110, 118, 158, 174, 190, 222, 254, 270, 286, 318, 350	15
	7 ETM+	22, 70, 230, 262, 278, 294, 326	7
2002	5 TM	11, 43, 59, 123, 155, 171, 187, 219, 235, 267, 283, 315, 331, 363	14
	7 ETM+	51, 115, 131, 147, 163, 179, 227, 243, 259, 323	10
2001	5 TM	24, 40, 72, 104, 120, 136, 152, 168, 200, 248, 264, 296, 312, 360	14
	7 ETM+	32, 80, 128, 144, 160, 208, 240, 272, 288, 320, 352,	11
2000	5 TM	6, 38, 70, 86, 102, 118, 134, 150, 166, 214, 262, 294, 358	13
	7 ETM+	46, 62, 78, 94, 110, 126, 142, 158, 206, 222, 254, 318, 334, 350	14

Average number of Landsat scenes for the above 11-year period is 23 scenes per year.

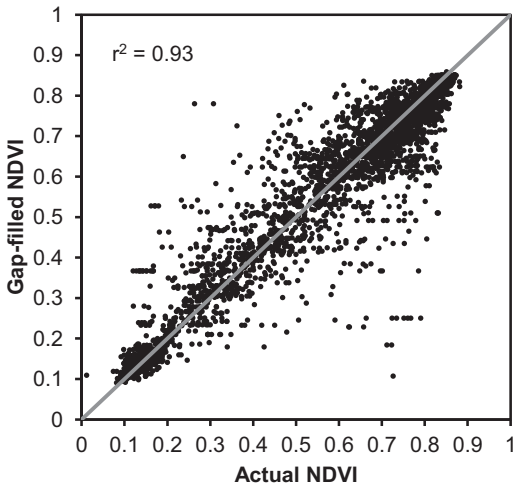

Fig. 3. Actual versus gap-filled NDVI values.

Gap-filling Landsat 7 missing NDVI data

We used multi-scale segmentation approach to fill missing NDVI data because it is easy to implement and was particularly suitable for filling missing pixels in agricultural lands (Maxwell et al., 2007; Zheng et al., 2013). The multi-scale segmentation approach assumes that values within an object (i.e., agricultural field in this case) are relatively homogeneous and uses object boundaries to guide the filling of missing values. We tailored the procedures used by Maxwell et al. (2007) and Zheng et al. (2013) to adapt to our local situations. A segmentation map was first generated to identify each object or field boundary with homogenous pixel values. Then the mean value of the valid pixels in the same object was used to fill the data gaps.

The segmentation map was produced using the multiresolution segmentation function (Baatz and Schäpe, 2000) in Definiens Developer 7 (Trimble Germany GmbH, Germany). Four Landsat 5 NDVI layers were selected as inputs to the segmentation algorithm. The NDVI layers were carefully chosen such that the boundaries of agricultural lands were easily discernible. The segmentation function hinges on three key parameters – scale, shape and compactness. Scale is a crucial parameter which determines the segmentation level, or more accurately, object size. Generally, a lower scale factor indicates higher segmentation level and produces smaller object size. A range of scale factors were tested and a scale of 10 was found effective in extracting the shape of agricultural lands without over segmentation. The shape parameter adjusts the balance between shape of objects and spectral homogeneity, whereas the compactness factor weighs compact edges versus smooth boundaries. Because spectral homogeneity plays the primary role in distinguishing different objects, the weighting on color was set to 0.9 and the shape factor was set to 0.1. Equal weights (0.5/0.5) were considered for compactness and smoothness, because the discrepancy was barely discernible, as we adjusted the compactness parameter.

We used a Landsat 5 TM NDVI image (DOY 049) with simulated missing data to evaluate the effectiveness of the gap-filling procedures. Five percent of gap-filled NDVI values were randomly sampled and compared to the actual NDVI values. The square of the correlation coefficient (R^2) and mean absolute differences between predicted and actual NDVI values were used to evaluate the predicted accuracy. The assessment results in an R^2 of 0.93 (Fig. 3) and a mean absolute difference of 0.04. Because of the effectiveness of the gap-filled procedures, we used the procedures to fill missing data for all the Landsat 7 images.

Detection of crop areas

We separated crop areas from non-crop areas by detecting changes in greenness using time-series NDVI data. Crop areas are cultivated agricultural lands. Non-crop areas include non-agricultural lands (such as water and urban) and uncultivated agricultural lands – fallow lands. Farm owners are required to maintain weed control on their fallow lands in the study area. Thus, even during the wet seasons, it is rare that fallow lands would appear as green as cultivated lands. Crop areas can be distinguished from non-crop areas by the dramatic changes in their greenness in our study area. Therefore, we extracted maximum and minimum NDVI values from the time-series imagery and calculated the percent difference between the maximum and the minimum NDVI. Pixels that have percent difference larger than 60% were classified as crop areas. Several large patches of natural vegetation along rivers and grasslands were also detected as crop areas, which were excluded manually. We then filtered 'salt and pepper' by removing any patches that have less than 20 neighboring pixels. Non-crop areas were then masked out from further analysis.

Training and validation data

Training and validation data come from three sources: local growers, USDA Farm Service Agency (FSA), and Cropland Data Layer (CDL) (USDA-NASS, 2010). A stratified-random sampling technique was used to sample 0.1% pixels from 2010 CDL for the following major crop types: alfalfa, cotton, corn, barley, wheat, wheat–sorghum double crops, and other crops. We visually assessed every time-series NDVI spectrum to verify the consistency between its spectral-temporal characteristics and the crop types reported by growers, FSA, and CDL data. Upon verification, there were a total of 553 samples (Table 2).

We mapped nine major crop categories (Table 2) and other crops. The nine major crop categories include six single crops (i.e., alfalfa, cotton, corn, wheat, barley, and potatoes) and three double crops (i.e., barley-cotton, wheat-sorghum, and wheat-cotton double crops) (Table 2). Because the training stage of a supervised classification could have a large impact on classification accuracy, we tested two different approaches for training set selection to assist identification of a better classification strategy. The first approach is specifically tailored to our local situation using prior knowledge of local farming practices in different irrigation districts, and designated as intelligent sample selection (Table 2). Given the fact that we have limited number of reference data for certain crop types, e.g., a total of five samples for barley–cotton (Table 2), and that certain crop types were practiced on a dozen or fewer agricultural fields, it is unwise to use dozens of samples for training for the 'rare' classes. Thus, only samples necessary for discrimination among spectrally similar classes are selected for training. Note that a single crop type can have more than one 'unique' spectrum. For instance, three different NDVI temporal profiles of barley (Fig. 4a and Table 2) are all included in the training dataset, but each is treated as an independent category in the training model. The number of training samples for each crop type was selected according to our best knowledge of local farming practices in different irrigation districts (Table 2). The second approach uses a stratified random sampling technique to sample a third of the entire samples without any human inputs (Table 2). Table 2 lists the number of training and validation data for each crop category using two different sampling strategies. A 60-m buffer was applied to the training categories that have only one sample to increase the number of pixels for these training groups (Table 2). Overall accuracy, kappa statistics, and user's and producer's

Table 2
The number of samples used for training and validation purposes.

	Crop type	Intelligent selection		Stratified random		Total
		Training	Validation	Training	Validation	
Single crops	Corn	2[a]	25	9	18	27
	Cotton	2[a]	99	33	68	101
	Barley	3[a]	23	9	17	26
	Wheat	1[a]	17	6	12	18
	Potatoes	1[a]	8	3	6	9
	Alfalfa	6[a]	252	83	175	258
Double crops	Barley/Cotton	1[a]	4	1[a]	4	5
	Wheat/Sorghum	2[a]	11	5	8	13
	Wheat/Cotton	1[a]	4	1[a]	4	5
	Other crops	24[a]	66	24[a]	66	90
	Total	44	509	174	378	553

[a] 60-m buffer was applied to increase the number of pixels.

accuracies were used to evaluate classification accuracy (Congalton and Green, 2008).

SVM classification

We used the LIBSVM (available from http://www.csie.ntu.edu.tw/~cjlin/libsvm/) for crop-type classification. The LIBSVM is an integrated tool for support vector classification and regression. The LIBSVM package (version 3.17) provides different SVM formulations, supports multi-class classification, and is embedded with a cross validation tool for model selection (Chang and Lin, 2011). We used the default SVM formulation, i.e., *C*-Support Vector Classification (*C*-SVC). Detailed mathematical formulations of *C*-SVC are available in Cortes and Vapnik (1995) and Chang and Lin (2011). The multi-class method uses a one-against-one (OAO) approach which first splits the classification into $n(n\text{-}1)/2$ binary models (n = number of classes), and then combines the outputs of each trained binary classifier using a majority voting strategy (Chih-Wei and Chih-Jen, 2002).

There are four basic kernel functions in SVM: linear, polynomial, radial basis function (RBF), and sigmoid. When the number of attributes is much smaller than the number of instances, one often maps data to higher dimensional spaces using nonlinear kernels to achieve an optimal result (Hsu et al., 2010). Thus, we used RBF kernel which can handle nonlinear relationship between class labels and attributes. RBF kernel parameters, penalty parameter C and gamma parameter γ, play an important role on decision boundary. C, also referred as the soft margin constant, creates a soft margin that permits some misclassifications (Ben-Hur and Weston, 2010). A small value of C permits ignorance of points close to the decision boundary and thus creates a large margin between classes (Ben-Hur and Weston, 2010). γ controls the 'smoothness' of the decision boundary. Increases in γ lead to greater curvature of the decision boundary (Ben-Hur and Weston, 2010). A large value of C and γ tends to classify training dataset accurately, but with a risk of overfitting, yielding a SVM model that could not generalize well to the rest of the data. Therefore, C and γ must be determined carefully to achieve the optimal generalization performance. We used a range of parameter values and 10-fold cross validation method to identify the best parameters C and γ for each training dataset. The parameters C and γ that achieve the highest overall accuracy are selected as the optimal parameters.

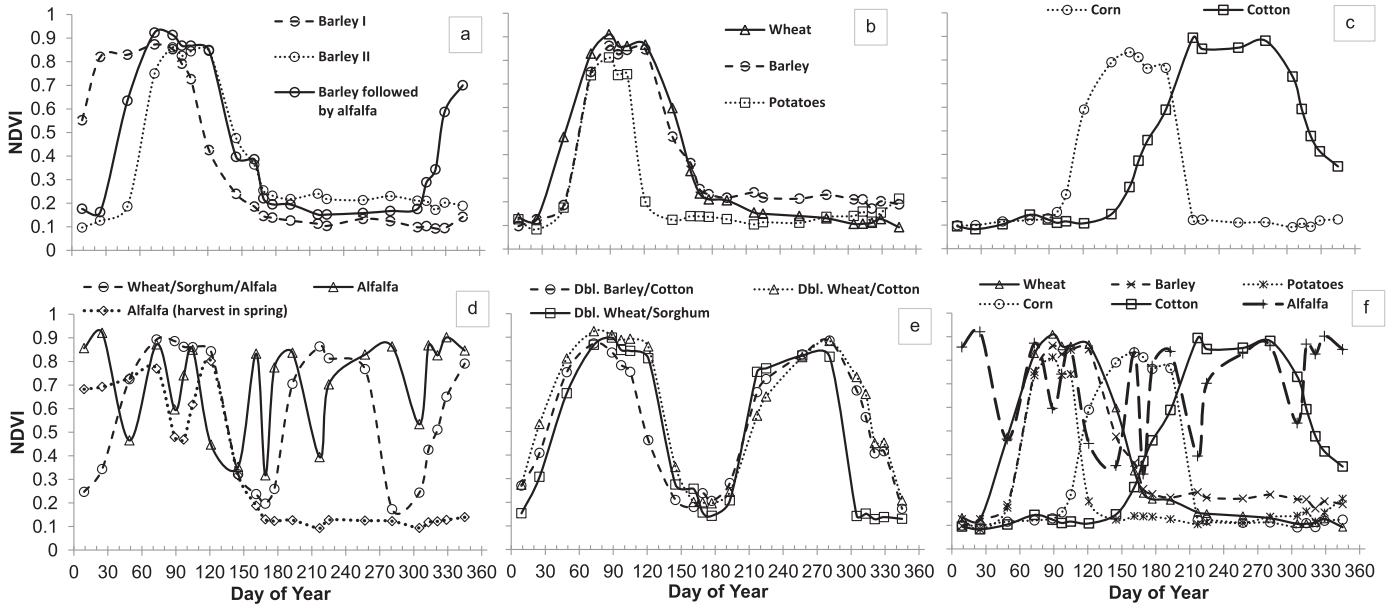

Fig. 4. Time-series NDVI spectral profiles for the major crop types planted in 2010: (a) varied planting dates causes different temporal spectral patterns for barley; (b) wheat, barley, and potatoes; (c) corn and cotton; (d) spring and full-year alfalfa and double crops wheat and sorghum followed by fall alfalfa; (e) double (Dbl.) crops: barley followed by cotton, wheat fallowed by cotton, and wheat followed by sorghum; (f) all six single crops are plotted together for comparison purposes.

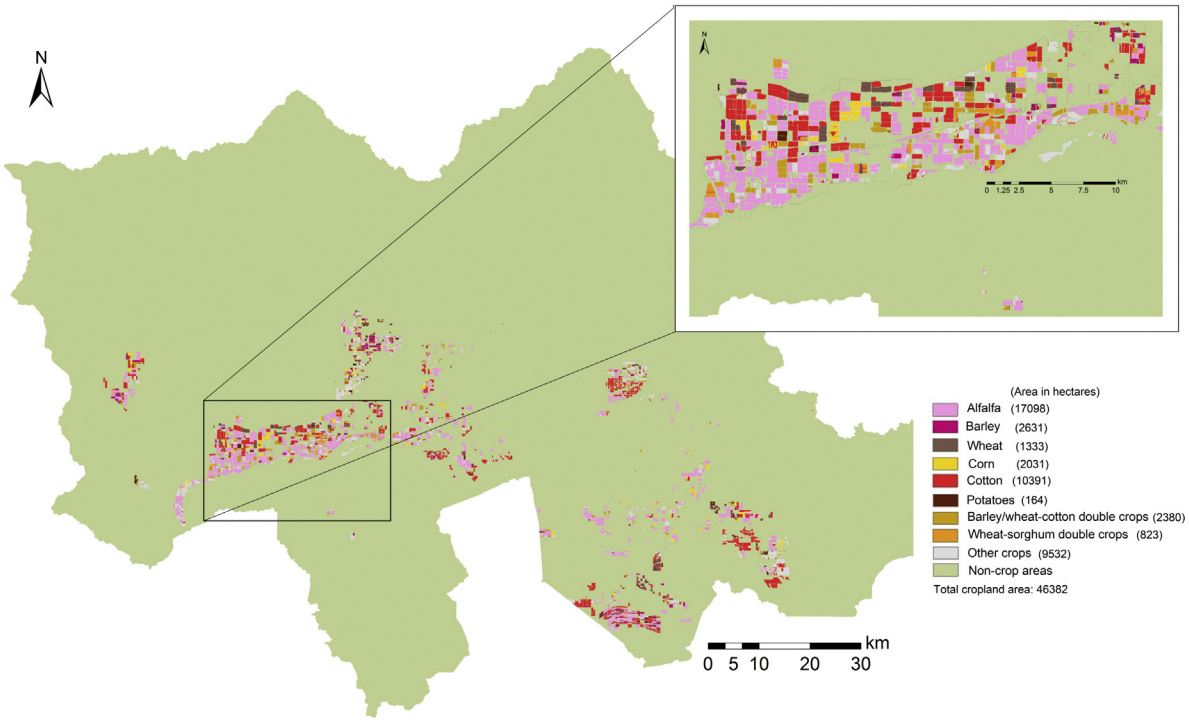

Fig. 5. 2010 crop type map for Phoenix Active Management Area (AMA). (For interpretation of the references to color in this figure legend, the reader is referred to the web version of this article.)

Spectral data of training and validation datasets were extracted from the time-series NDVI image using ENVI 5.0 (Exelis Visual Information Solutions, Boulder, Colorado) and then reformatted into LIBSVM format using a script developed in MATLAB (The MathWorks Inc., Natick, MA). We firstly applied 10-fold cross validation method to the training datasets to select the best parameters C and γ. The training datasets and the selected parameters were then used to develop SVM models, which were applied to the validation datasets to examine their predictive abilities.

Results and discussion

Crop phenological curves

The abundant number of cloud-free Landsat observations for our study area permits comparison of phenological patterns among different crop types. Fig. 4 shows time-series NDVI spectral profiles for the major crops planted in 2010. Phenological curves could vary for the same type of crop from one farm to another, depending on planting dates, variety, weather, soil conditions, and crop management. For example, barley can start emerging any time in December, January, and February depending on individual growers' planting schedules (Fig. 4a). Durum wheat and barley have similar phenological patterns (Fig. 4b). They are planted in late November through mid-January, and harvested in late April to mid-May (Fig. 2). In general, barley is harvested several days earlier than durum wheat, and durum wheat's peak NDVI is higher than barley's (Figs. 2 and 4b). Potatoes are harvested earlier than barley and wheat and the length of growing period is shorter. Thus, potatoes are spectrally separable from wheat and barley (Fig. 4b).

Planting dates of summer crops can be from March to April or during the summer from June to July for sorghum, from March to April for corn, and from March to June for cotton. In general, sorghum is sown later than corn planting, while corn is planted and harvested earlier than cotton. Fig. 3c shows that the spectral patterns of corn and cotton are separable. Fields planted with alfalfa stay green throughout or nearly throughout the year with all the NDVI values higher than 0.3 (Fig. 4d). Alfalfa is the most common crop in the area which grows continuously for three or four years before rotating to the other crops. On average, it can be cut eight times or more over the year (Fig. 4d). Most growers in this region rotate between alfalfa and small grain crops, corn, cotton, or sorghum. It is common that they grow small grain crops for two years fallowed by three to four years of alfalfa. The optimum planting date for alfalfa is October in this area with a planting time window from October to March. Thus, greening in the late fall (mid-October and November) is generally caused by the emerging alfalfa, such as barley fallowed by alfalfa (Fig. 4a) and wheat-sorghum double crops followed by alfalfa (Fig. 4d). The greening in the late fall could also be due to fall/winter vegetables which are grown in the Maricopa Irrigation District and northern area of Salt River Pima-Maricopa Indian Community. Single/double crops followed by fall alfalfa are not considered as double/triple crops because fall alfalfa is not harvested until next year. Growers may harvest the third or fourth year alfalfa in the spring and let the field fallow for the rest of the year depending on the condition of the alfalfa (Fig. 4d). Sorghum, corn, or cotton can be planted right after the harvest of spring crops on the same field. It is common for growers to practice double cropping in the study area (Fig. 4d and e). Double cropping could be any combinations of spring, summer, and/or fall crops.

Fig. 4 shows the time-series NDVI spectra of typical crop types to reveal various cropping patterns in our study area. In contrast to the Mid-West, where temporal coverage from April to October is sufficient for crop identification, a series of continuous, full-year satellite observations is required to acquire accurate information of cropping practices in Arizona due to year-round farming practices (Fig. 4). The readily available CDL data for Arizona mainly utilizes satellite images acquired from April to October (USDA-NASS, 2013). The image time window from April to October does not cover the entire growing season, and hence, could potentially introduce classification errors, because it is unable to detect any crops grown between January and April or between October and December. For

instance, potato fields harvested in early April are likely classified as fallow lands when no image from the potato's growing period was used for classification. The incomplete time window also increases the risk of misclassification between single and double crops.

SVM classifications

The 10-fold cross validation resulted in the best penalty parameter C of 16 and gamma parameter γ of 0.25 for the SVM model using the 44 training samples selected intelligently. Accuracy assessment on the validation dataset shows overall accuracy of 90%, kappa coefficient is 85%, and >57% user's and producer's accuracy for all classes (Table 3). Both user's and producer's accuracies are relatively low for wheat and barley, while user's accuracy of barley–cotton (57%) and wheat–sorghum (71%) double crops is also lower than other classes. Most misclassification happened between wheat and barley due to the spectral similarity between them. Onset of greenness of wheat and barley varies across the study area depending on growers' schedules and preferences in crop managements. Although the maximum NDVI (peak greenness) values and the length of growing season of wheat are usually higher than those of barley, they also vary according to different soil fertility and farm management practices. One pixel was misclassified as potatoes for both wheat and barley (Table 3) because time-series NDVI profiles of barley/wheat could be spectrally similar to those of potatoes as a result of poor crop conditions. While maximum likelihood classification uses class mean and covariance of training samples as inputs, SVMs only uses training samples that lie on the edge of the class distribution in feature space. Therefore, training samples that lie on the class boundaries are particularly useful for forming an accurate hyperplane to discriminate classes for SVM classification (Foody and Mathur, 2004). Samples that lie on the class boundaries are more spectrally similar than those that lie away from the class boundary. Thus, the two spectrally similar, misclassified pixels, could be included in the training data to maximize discrimination between the poorly-grown barley/wheat and potatoes pixels. Twenty-two alfalfa pixels were misclassified as other crops, indicating that the support vectors were not well specified between alfalfa and other crops. The study area is dominated with alfalfa crops, and spectral profiles of alfalfa differ from one field to another due to varied timings of the cuttings. Thus, increases in the number of alfalfa training samples could potentially improve the ability of SVM model to find the optimal hyperplanes. A careful sample selection of other crops is as important as that of the major crops. Otherwise, the classification algorithm could easily misclassify other crops as the major crop types and lower the user's classification accuracy. The number of validation samples is limited for several classes, especially for potatoes and double crops which have less than 12 samples. Thus, the resulting high producer's and user's accuracies (100%) of these crop types may not well represent the 'true' classification accuracy, and a larger validation sample size will enable a more reliable assessment of the classification accuracy.

The optimal penalty parameter C of 32 and gamma parameter γ of 0.25 were yielded for the SVM model using the 10-fold cross validation and training samples selected by stratified random sampling. The SVM model results in overall accuracy of 86%, kappa coefficient of 80%, >43% user's accuracy, and >67% producer's accuracy (Table 4). The producer's accuracy of alfalfa was improved from 88% to 97% by including more alfalfa samples in the training dataset (Tables 3 and 4). In addition, including more samples of barley and wheat in the training generated a more accurate hyperplane to discriminate them from potatoes. However, the stratified random sampling technique resulted in lower classification accuracy for the other classes. The degraded performance could be caused by the less informative training samples

Table 3
Error matrix for the support vector machine classification with the training samples selected intelligently – a total of 44 training samples.

Reference												
Classification	Single crops						Double crops			Other crops	Total	User's accuracy %
	Corn	Cotton	Wheat	Barley	Potatoes	Alfalfa	Barley/Cotton	Wheat/Sorghum	Wheat/Cotton			
Corn	**24**									1	25	96
Cotton		**99**								6	105	94
Wheat			**13**	7							20	65
Barley			3	**13**		1					17	76
Potatoes			1	1	**8**						10	80
Alfalfa						**223**					223	100
Barley/Cotton						2	**4**	1			7	57
Wheat/Sorghum						4		**9**			14	71
Wheat/Cotton									**4**		4	100
Other crops	1			2		22				**59**	84	70
Total	25	99	17	23	8	252	4	11	4	66	509	
Producer's accuracy %	96	100	76	57	100	88	100	91	100	89		

Overall accuracy: 90%; kappa statistic: 85%.
Bold data are the number of pixels correctly assigned to each class.
Note: Taken wheat as an example, as a producer, 76% of the wheat pixels (in reference) are correctly classified as wheat by SVM algorithm. As a user, 65% of the pixels classified as wheat (by SVM algorithm) are indeed wheat.

Table 4
Error matrix for the support vector machine classification with the stratified random samples – a total of 174 training samples.

Reference												
Classification	Single crops						Double crops			Other crops	Total	User's accuracy %
	Corn	Cotton	Wheat	Barley	Potatoes	Alfalfa	Barley/Cotton	Wheat/Sorghum	Wheat/Cotton			
Corn	**15**									7	22	68
Cotton	1	**66**								8	75	88
Wheat			**8**	7							15	53
Barley			4	**10**							14	71
Potatoes	1				**6**						7	85
Alfalfa						**170**				12	182	93
Barley/Cotton						1	**3**	3			7	43
Wheat/Sorghum						1		**5**			6	83
Wheat/Cotton		1					1		**4**		6	67
Other crops	1	1				3				**39**	44	89
Total	18	68	12	17	6	175	4	8	4	66	378	
Producer's accuracy %	96	97	67	59	100	97	75	63	100	59		

Overall accuracy: 86%; kappa statistic: 80%.
Bold data are the number of pixels correctly assigned to each class.
Note: Taken wheat as an example, as a producer, 67% of the wheat pixels (in reference) are correctly classified as wheat by SVM algorithm. As a user, 53% of the pixels classified as wheat (by SVM algorithm) are indeed wheat.

selected without human knowledge inputs. Another possibility could be biases introduced by the imbalanced data generated by the stratified random sampling technique (Ben-Hur and Weston, 2010). The Synthetic Minority Over-sampling Technique (SMOTE) is a powerful method to improve generalization of many machine learning models (Chawla et al., 2002). The SMOTE generates synthetic samples of the minority class using nearest neighbors of these minority classes to achieve a more balanced dataset (Chawla et al., 2002). We incorporated the SMOTE method to examine whether a more balanced dataset can improve the classification accuracy. The SVM of the SMOTE dataset resulted in an overall accuracy of 86%. Therefore, our experiment showed that a more balanced dataset did not improve the performance of the SVM model. Possible reasons could be: (1) SVMs can achieve relatively robust classification accuracy when applied to imbalanced data (Japkowicz and Stephen, 2002); (2) multiclass OAO approach is more effective for imbalanced datasets than one-against-all (OAA) approach because each binary SVM is trained with class i data against class j data unless these two classes have imbalanced data (Ou and Murphey, 2007). In addition, the independent trained binary SVMs from the OAO approach provide redundancy to the prediction of pattern classes. Because of the redundancy, the feature space is less likely to have uncovered areas as indicated in the OAA modeling approach, and as a result, the OAO method can be used to improve model generalization (Ou and Murphey, 2007).

Classification accuracy is generally higher using the training samples selected intelligently than using those selected by the stratified random sampling technique. The intelligent sample selection method is particularly useful when there is limited availability of ground reference data, and when a composite of various crop types is present within a small geographical area. The training stage using the stratified random sampling technique is much faster than using the intelligent selection technique because it requires no prior human knowledge. However, the trained SVM model using the stratified random samples could not generalize as well as the one using the intelligent selected samples. Selecting training sets via random sampling works well with a large reference data (Peña-Barragán et al., 2011; Shao and Lunetta, 2012), but is not optimal when there are classes with only a few samples. The classification map (Fig. 5) using the 44 spectral classes is particularly useful for annual crop evapotranspiration/agricultural water use assessments because spectra with and without fall alfalfa (Fig. 4) are treated as individual classes. Annual crop evapotranspiration is expected to be higher for fields planted with the same crop types fallowed with alfalfa in the fall than those without. The high classification accuracy also contributed to the good sequence of Landsat observations, which permit good separability among various classes (Fig. 4). Double cropping patterns were successfully identified using the time-series Landsat NDVI image, although misclassification exists among different double crops (Tables 3 and 4).

Our study area has plenty of cloud-free/near cloud-free Landsat observations for years from 2000 to 2009 with an average of 23 scenes per year (Table 1). Consequently, crop types can be systematically monitored using SVM of time-series Landsat data. A detail crop-type map with many classes may yield lower classification accuracy compared to multiple-class crop-type maps. Considering water consumption of barley and wheat is similar, it is reasonable to group barley and wheat together as one class for agricultural water use assessment. Subsequently, classification accuracy will be improved for a seven-class classification: alfalfa, corn, cotton, potatoes, small grains (i.e., wheat and barley), small grain–cotton double crops, and wheat–sorghum double crops. Nevertheless, our results demonstrated that SVM of time-series Landsat data is capable of identifying different crop types.

Conclusions

We tested the capability of support vector machines (SVMs) to discriminate nine major crop types in a complex cropping system using limited number of training samples and time-series Landsat imagery. While a sequence of images collected from April to October (USDA-NASS, 2013) can only capture a portion of the cropping practices, a temporal coverage of Landsat imagery from January to December is necessary for accurate crop classification for our study area, where crops are grown year round. Our results showed that the SVM hyperplanes generated from the small intelligently selected training samples generalized well to the rest of the data with overall classification accuracy of 90% for the nine major crop types. The producer's and user's accuracies varied between 57 and 100% for the nine crops. Greatest difficulty was in separating wheat from barley since both have similar erectophile structure as well as phenological growth phases. When ground reference data is limited, knowledge of local farming practices is particularly important for identifying informative training samples to achieve better classification accuracy. We provided the information on crop calendar and crop spectral-temporal profiles to assist the selection of informative training sets to distinguish different crop types for this region. Future investigation on how crop spectral-temporal profiles vary over time will facilitate operational implementation of crop type mapping. Abundant numbers of cloud-free Landsat imagery in drylands, deserts, and desertified areas in semi-arid, arid, and any dry climate regions provide multiple opportunities for monitoring croplands systematically using Landsat imagery alone.

Acknowledgments

The study was funded by National Oceanic and Atmospheric Administration (grant number: NA12OAR4310100). The authors would like to thank Christina Day (Maricopa County Farm Service Agency) and several local growers, including Mr. Ron Rayner, Mr. Adam Hatley, Mr. Marvin John, Mr. Steve Sossaman, Mr. W.T. Gladden, and Mr. Brandon Brooks for providing ground reference data. We also would like to thank the supports by National Science Foundation under grant number BCS-1026865 for Central Arizona-Phoenix Long-Term Ecological Research (CAPLTER), and grant numbers SES-0951366 & SES-0345945 for Decision Center for a Desert City (DCDC).

References

ADWR, 2012a. Active Management Area Climate, Retrieved from http://www.azwater.gov/AzDWR/StatewidePlanning/WaterAtlas/ActiveManagementAreas/PlanningAreaOverview/Climate.htm (accessed 28.08.13).

ADWR, 2012b. Phoenix AMA Cultural Water Demand, Retrieved from http://www.azwater.gov/AzDWR/StatewidePlanning/WaterAtlas/ActiveManagementAreas/Cultural/PhoenixAMA.htm (accessed 28.08.13).

Baatz, M., Schäpe, A., 2000. Multiresolution segmentation: an optimization approach for high quality multi-scale image segmentation. In: Strobl, J. (Ed.), Angewandte Geographische Informationsverarbeitung XII. Beiträge zum AGIT-Symposium Salzburg 2000. Herbert Wichmann Verlag, Karlsruhe, pp. 12–23.

Belousov, A.I., Verzakov, S.A., von Frese, J., 2002. A flexible classification approach with optimal generalisation performance: support vector machines. Chemom. Intell. Lab. Syst. 64, 15–25.

Ben-Hur, A., Weston, J., 2010. A user's guide to support vector machines. In: Carugo, O., Eisenhaber, F. (Eds.), Data Mining Techniques for the Life Sciences. Humana Press, pp. 223–239.

Brown, M., Lewis, H.G., Gunn, S.R., 2000. Linear spectral mixture models and support vector machines for remote sensing. IEEE Trans. Geosci. Remote Sens. 38, 2346–2360.

Bruzzone, L., Persello, C., 2009. A novel context-sensitive semisupervised SVM classifier robust to mislabeled training samples. IEEE Trans. Geosci. Remote Sens. 47, 2142–2154.

Carrão, H., Gonçalves, P., Caetano, M., 2008. Contribution of multispectral and multitemporal information from MODIS images to land cover classification. Remote Sens. Environ. 112, 986–997.

CAST, 2009. Water, People, and the Future: Water Availability for Agriculture in the United States, Issue Paper 44. Council for Agricultural Science and Technology (CAST), Ames, IA.

Chang, C.-C., Lin, C.-J., 2011. LIBSVM: a library for support vector machines. ACM Trans. Intell. Syst. Technol. 2, 1–27.

Chang, J., Hansen, M.C., Pittman, K., Carroll, M., DiMiceli, C., 2007. Corn and soybean mapping in the United States using MODIS time-series data sets. Agron. J. 99, 1654–1664.

Chawla, N.V., Bowyer, K.W., Hall, L.O., Kegelmeyer, W.P., 2002. SMOTE: synthetic minority over-sampling technique. J. Artif. Intell. Res. 16 (1), 321–357.

Chih-Wei, H., Chih-Jen, L., 2002. A comparison of methods for multiclass support vector machines. IEEE Trans. Neural Netw. 13, 415–425.

Congalton, R.G., Green, K., 2008. Assessing the Accuracy of Remotely Sensed Data: Principle and Practices, 2nd ed. Levis Publishers, Boca Raton, FL.

Cortes, C., Vapnik, V., 1995. Support-vector networks. Mach. Learn. 20 (3), 273–297, http://dx.doi.org/10.1023/a:1022627411411.

Cousteau, J., 2012. We Forget that the Water Cycle and the Life Cycle are One. Arizona Department of Water Resources (ADWR), Retrieved from http://www.azwater.gov/AzDWR/StatewidePlanning/Conservation2/Agriculture/ (accessed 28.08.13).

Dalponte, M., Bruzzone, L., Gianelle, D., 2008. Fusion of hyperspectral and LIDAR remote sensing data for classification of complex forest areas. IEEE Trans. Geosci. Remote Sens. 46, 1416–1427.

Foody, G.M., Mathur, A., 2004. Toward intelligent training of supervised image classifications: directing training data acquisition for SVM classification. Remote Sens. Environ. 93, 107–117.

Gleick, P.H., Palaniappan, M., 2010. Peak water limits to freshwater withdrawal and use. Proc. Natl. Acad. Sci. U. S. A. 107, 11155–11162.

Hsu, C.-W., Chang, C.-C., Lin, C.-J., 2010. A Practical Guide to Support Vector Classification, Retrieved from http://www.csie.ntu.edu.tw/~cjlin/papers/guide/guide.pdf (accessed 20.09.2013).

Impacts of Agricultural Production, 2010. Impacts of Agricultural Production and Specialty Crops on Arizona's Economy in 2007, Initial Report. Department of Agricultural and Resource Economics, The College of Agriculture and Life Sciences, The University of Ariziona, pp. 33.

Japkowicz, N., Stephen, S., 2002. The class imbalance problem: a systematic study. Intell. Data Anal. 6 (5), 429–449.

Karl, T.R., Melillo, J., Peterson, T., 2009. Global Climate Change Impacts in the United States. Cambridge University Press, Cambridge, UK.

Long, J.A., Lawrence, R.L., Greenwood, M.C., Marshall, L., Miller, P.R., 2013. Object-oriented crop classification using multitemporal ETM+SLC-off imagery and random forest. GISci. Remote Sens. 50, 418–436.

Löw, F., Michel, U., Dech, S., Conrad, C., 2013. Impact of feature selection on the accuracy and spatial uncertainty of per-field crop classification using support vector machines. ISPRS J. Photogram. Remote Sens. 85, 102–119.

Masek, J.G., Vermote, E.F., Saleous, N.E., Wolfe, R., Hall, F.G., Huemmrich, K.F., Feng, G., Kutler, J., Teng-Kui, L., 2006. A Landsat surface reflectance dataset for North America, 1990–2000. IEEE Geosci. Remote Sens. Lett. 3, 68–72.

Maxwell, S.K., Schmidt, G.L., Storey, J.C., 2007. A multi-scale segmentation approach to filling gaps in Landsat ETM+SLC-off images. Int. J. Remote Sens. 28, 5339–5356.

Mountrakis, G., Im, J., Ogole, C., 2011. Support vector machines in remote sensing: a review. ISPRS J. Photogram. Remote Sens. 66, 247–259.

Ou, G., Murphey, Y.L., 2007. Multi-class pattern classification using neural networks. Pattern Recognit. 40 (1), 4–18, http://dx.doi.org/10.1016/j.patcog.2006.04.041.

Overpeck, J., Udall, B., 2010. Dry times ahead. Science 328, 1642–1643.

Peña-Barragán, J.M., Ngugi, M.K., Plant, R.E., Six, J., 2011. Object-based crop identification using multiple vegetation indices, textural features and crop phenology. Remote Sens. Environ. 115, 1301–1316.

Plaza, A., Benediktsson, J.A., Boardman, J.W., Brazile, J., Bruzzone, L., Camps-Valls, G., Chanussot, J., Fauvel, M., Gamba, P., Gualtieri, A., Marconcini, M., Tilton, J.C., Trianni, G., 2009. Recent advances in techniques for hyperspectral image processing. Remote Sens. Environ. 113 (Suppl. 1), S110–S122.

Serra, P., Pons, X., 2008. Monitoring farmers' decisions on Mediterranean irrigated crops using satellite image time series. Int. J. Remote Sens. 29, 2293–2316.

Shao, Y., Lunetta, R.S., 2012. Comparison of support vector machine, neural network, and CART algorithms for the land-cover classification using limited training data points. ISPRS J. Photogram. Remote Sens. 70, 78–87.

Shao, Y., Lunetta, R.S., Ediriwickrema, J., Iiames, J., 2010. Mapping cropland and major crop types across the Great Lakes Basin using MODIS-NDVI data. Photogram. Eng. Remote Sens. 75, 73–84.

Sheppard, P.R., Comrie, A.C., Packin, G.D., Angersbach, K., Hughes, M.K., 2002. The climate of the US Southwest. Clim. Res. 21, 219–238.

Thenkabail, P.S., Wu, Z., 2012. An automated cropland classification algorithm (ACCA) for Tajikistan by combining Landsat, MODIS, and secondary data. Remote Sens. 4, 2890–2918.

Thenkabail, P.S., Knox, J.W., Ozdogan, M., Gumma, M.K., Congalton, R.G., Wu, Z., Milesi, C., Finkral, A., Marshall, M., Mariotto, I., You, S., Giri, C., Nagler, P., 2012. Assessing future risks to agricultural productivity, water resources and food security: how can remote sensing help? Photogram. Eng. Remote Sens. 78, 773–782.

Turker, M., Arikan, M., 2005. Sequential masking classification of multi-temporal Landsat 7 ETM+images for field-based crop mapping in Karacabey, Turkey. Int. J. Remote Sens. 26, 3813–3830.

USDA-NASS, 2004. Arizona Field Office 2004 Annual Statistics Bulletin, Retrieved from http://www.nass.usda.gov/Statistics_by_State/Arizona/Publications/Bulletin/04bul/main.htm (accessed 25.11.13).

USDA-NASS, 2010. Arizona Cropland Data Layer. USDA-NASS, Retrieved from http://www.nass.usda.gov/research/Cropland/metadata/metadata_az10.htm (accessed 17.09.13).

USDA-NASS, 2013. Cropland Data Layer Metadata. USDA-NASS, Retrieved from http://www.nass.usda.gov/research/Cropland/metadata/meta.htm (accessed 17.09.13).

USDA-NRCS, 2013. Land Resource Regions and Major Land Resource Areas of the United States, the Caribbean, and the Pacific Basin – MLRA 40, Retrieved from http://soils.usda.gov/MLRAExplorer (accessed 17.09.13).

Vapnik, V.N., 1999. The Nature of Statistical Learning Theory, 2nd ed. Springer, New York, NY.

Vintrou, E., Desbrosse, A., Bégué, A., Traoré, S., Baron, C., Lo Seen, D., 2012. Crop area mapping in West Africa using landscape stratification of MODIS time series and comparison with existing global land products. Int. J. Appl. Earth Obs. Geoinf. 14, 83–93.

Wardlow, B.D., Egbert, S.L., 2008. Large-area crop mapping using time-series MODIS 250 m NDVI data: an assessment for the U.S. Central Great Plains. Remote Sens. Environ. 112, 1096–1116.

Wardlow, B.D., Egbert, S.L., Kastens, J.H., 2007. Analysis of time-series MODIS 250 m vegetation index data for crop classification in the U.S. Central Great Plains. Remote Sens. Environ. 108, 290–310.

Zheng, B., Campbell, J.B., Shao, Y., Wynne, R.H., 2013. Broad-scale monitoring of tillage practices using sequential Landsat imagery. Soil Sci. Soc. Am. J. 77 (5), 1755–1764.

Zhong, L., Gong, P., Biging, G.S., 2014. Efficient corn and soybean mapping with temporal extendability: a multi-year experiment using Landsat imagery. Remote Sens. Environ. 140, 1–13.